Eur. Phys. J. B **45**, 449–454 (2005)
DOI: 10.1140/epjb/e2005-00216-2

THE EUROPEAN PHYSICAL JOURNAL B

Curie temperature in the Hubbard model with alloy disorder

K. Byczuk[1,a] and M. Ulmke[2]

[1] Institute of Theoretical Physics, Warsaw University, ul. Hoża 69, 00-681 Warszawa, Poland
[2] FGAN - FKIE, Neuenahrer Strasse 20, 53343 Wachtberg, Germany

Received 14 January 2005 / Received in final form 25 March 2005
Published online 13 July 2005 – © EDP Sciences, Società Italiana di Fisica, Springer-Verlag 2005

Abstract. Magnetic and electric properties of the Hubbard model with binary alloy disorder are studied within the dynamical mean-field theory. A paramagnet-ferromagnet phase transition and a Mott-Hubbard metal-insulator transition are observed upon varying the alloy concentration. A disorder induced enhancement of the Curie temperature is demonstrated and explained by the effects of band splitting and subband filling.

PACS. 71.10.-w Theories and models of many-electron systems – 71.10.Fd Lattice fermion models (Hubbard model, etc.) – 71.27.+a Strongly correlated electron systems; heavy fermions

1 Introduction

There is a great concern about the nature of itinerant ferromagnetism in correlated electron systems with disorder, such as, e.g., doped manganites ($La_{1-x}Sr_xMnO_3$) [1,2], alloyed ruthenates ($SrRu_{1-x}Mn_xO_3$) [3], or alloyed Kondo insulators ($FeSi_{1-x}Ge_x$) [4,5]. Moreover, it is of fundamental importance for industrial applications to precisely control the Curie temperature of different ferromagnetic alloys or diluted magnetic semiconductors, e.g. $Ga_{1-x}Mn_xAs$ [6,7].

In typical transition metals (e.g. Fe, Ni or Co) the subtle competition between kinetic and Coulomb energies together with the Pauli principle leads to the occurrence of a ferromagnetic phase. Since the transition happens when both contributions to the total energy are of the same order, theoretical methods to study such systems have to be nonperturbative [8]. Within the dynamical mean-field theory (DMFT) [9–11] detail conditions for occurrence of ferromagnetism in a one-band Hubbard model were elucidated [12,13]. The same nonperturbative scheme together with a density functional theory in the local density approximation was used to describe ferromagnetic phases of Fe and Ni [14]. The presence of a binary alloy disorder introduces a new nonperturbative aspect into the problem. Namely, when the difference between ion energies Δ is larger then the band-width W, the conducting band is split and two alloy subbands are formed [15].

Recent investigation of the one-band Hubbard model with a binary alloy disorder demonstrated an intriguing interplay between effects due to interaction and randomness [16]. It was shown in reference [16] that for electron densities $n < x$, where x was a fixed concentration of an alloy ion, and for large local Coulomb interactions U the Curie temperature T_c is enhanced when Δ is increased. Additionally, at $n = x$ the Mott-Hubbard metal-insulator transition (MIT) occurs for $\Delta = \Delta_c(U)$. The Mott-Hubbard transition in a non-integer filled system with binary alloy disorder was investigated further in reference [17] where the notions of an *alloy Mott insulator* ($\Delta > U$) and an *alloy charge-transfer insulator* ($\Delta < U$) were introduced.

In the present paper we study the one-band Hubbard model and determine its physical properties, such as the Curie temperature, as a function of x. The Mott-Hubbard MIT can be reached by varying x while n, Δ and U are constants. Such MIT will be called an *alloy concentration controlled* Mott transition. This notion extends the previous classification of *band-width controlled* and *filling controlled* Mott transitions [1]. As will be presented below, under certain circumstances the Curie temperature has a maximum at a finite alloy concentration. All those effects, as explained below, are caused by a subtle interplay between alloy band splitting and correlations.

The present work is motivated by real experimental situations where the tuning parameter is rather x than Δ. Namely, while the latter is fixed for given atoms the former can be varied by making different alloy compositions or changing chemical stoichiometry. Thereby, the controlling of Curie temperature $T_c(x)$ is experimentally accessible. The examples are bcc Fe-Co or fcc Ni-Cu alloys [18,19]. In the first case, due to alloying, the system is driven from weak to strong ferromagnetism, whereas in the latter case the system is changed from a ferromagnet to a paramagnet. Interestingly, the behavior of the saturated magnetization and the Curie temperature in Fe-Co are non-monotonous functions of x reaching maxima at 30% concentration of Co [18]. Other interesting

[a] e-mail: byczuk@fuw.edu.pl

examples are pyrite alloys $T_{1-x}T'_xS_2$, where T (T') stands for transition metals: Fe, Co, Ni, Cu, Zn [20]. Starting from FeS_2 and alloying it with Co, the empty e_g band (FeS_2 is a narrow-band semiconductor) is progressively filled in with electrons and the system becomes a disordered itinerant ferromagnet. Surprisingly, the maximum $T_c(x)$ in $Fe_{1-x}Co_xS_2$ occurs not at $x = 1$ but at $x \approx 0.76$. In different compound $UCu_2Si_{2-x}Ge_x$ the Curie temperature has a maximum at $x \approx 1.6$, i.e. again when the system is disordered [21]. Interesting aspect of this alloy is that since Si and Ge are isovalent, the system is isoelectronic and the disorder has only structural character not influencing directly the magnetic arrangement.

In Section 2 we introduce a one-band Anderson-Hubbard model with quenched binary alloy disorder and solve it within DMFT framework. In Section 3 we present our results on ferromagnetic properties of this model when the density of electrons is independent of alloy concentration, i.e. the system is isoelectronic when x is varied. Next, in Section 4 we discuss our results when the system is non-isoelectronic under the change of x. Section 5 presents conclusions and a final discussion.

2 Model and dynamical mean-field theory

2.1 Anderson-Hubbard Hamiltonian

Itinerant electron ferromagnetism in binary alloy is described hereby the Anderson-Hubbard Hamiltonian with uncorrelated on-site disorder

$$H = \sum_{ij,\sigma} t_{ij}\hat{c}^+_{i\sigma}\hat{c}_{j\sigma} + \sum_{i\sigma}\epsilon_i\hat{n}_{i\sigma} + U\sum_i \hat{n}_{i\uparrow}\hat{n}_{i\downarrow}, \qquad (1)$$

where t_{ij} is the hopping matrix element, U is the local Coulomb interaction, $\hat{c}^+_{i\sigma}$ is the fermionic creation operator for an electron with spin σ in Wannier state i, and $\hat{n}_{i\sigma}$ is the particle number operator. The quenched disorder is represented by the atomic energies ϵ_i, which are random variables. We consider binary alloy disorder where the atomic energy is distributed according to the binomial probability density

$$P(\epsilon_i) = x\delta\left(\epsilon_i + \frac{\Delta}{2}\right) + (1-x)\delta\left(\epsilon_i - \frac{\Delta}{2}\right). \qquad (2)$$

Here Δ is the energy difference between the two atomic energies, providing a measure of the disorder strength, while x and $1-x$ are the concentrations of the two alloy atoms. For $\Delta \gg W$, where W is the band-width, it is known that binary alloy disorder causes a band splitting [15]. The number of states in each alloy subband is equal to $2xN_a$ and $2(1-x)N_a$, respectively, where N_a is the number of lattice sites and a factor two counts the spin degeneracy.

2.2 Dynamical mean-field theory

The Anderson-Hubbard Hamiltonian (1) is not solvable at any finite space dimension. It is however numerically solvable in an infinite dimension after a proper rescaling of the hopping parameters [22], i.e. a set of self-consistent DMFT equations is derived [9–11]. The local nature of the theory implies that short-range order in position space is missing. However, dynamical correlations due to the local interaction and disorder [23,24] are fully taken into account.

In the DMFT scheme the local Green function $G_{\sigma n}$ is given by the bare density of states $N^0(\epsilon)$ and the local self-energy $\Sigma_{\sigma n}$ as

$$G_{\sigma n} = \int d\epsilon \frac{N^0(\epsilon)}{i\omega_n + \mu - \Sigma_{\sigma n} - \epsilon}. \qquad (3)$$

Here the subscript n refers to the Matsubara frequency $\omega_n = (2n+1)\pi/\beta$ for the temperature T, with $\beta = 1/k_BT$, and μ is the chemical potential. Within DMFT the local Green function $G_{\sigma n}$ is determined self-consistently by

$$G_{\sigma n} = -\left\langle \frac{\int D\left[c_\sigma, c^\star_\sigma\right] c_{\sigma n} c^\star_{\sigma n} e^{\mathcal{A}_i\{c_\sigma, c^\star_\sigma, \mathcal{G}^{-1}_\sigma\}}}{\int D\left[c_\sigma, c^\star_\sigma\right] e^{\mathcal{A}_i\{c_\sigma, c^\star_\sigma, \mathcal{G}^{-1}_\sigma\}}} \right\rangle_{\rm dis}, \qquad (4)$$

together with the $\mathbf{k}$-integrated Dyson equation

$$\mathcal{G}^{-1}_{\sigma n} = G^{-1}_{\sigma n} + \Sigma_{\sigma n}. \qquad (5)$$

The single-site action $\mathcal{A}_i$ for a site with the ionic energy $\epsilon_i = \pm\Delta/2$ for $i =$A and B, respectively, has the form

$$\mathcal{A}_i\{c_\sigma, c^\star_\sigma, \mathcal{G}^{-1}_\sigma\} = \sum_{n,\sigma} c^\star_{\sigma n}\mathcal{G}^{-1}_{\sigma n}c_{\sigma n} - \epsilon_i\sum_\sigma \int_0^\beta d\tau n_\sigma(\tau) - \frac{U}{2}\sum_\sigma \int_0^\beta d\tau c^*_\sigma(\tau)c_\sigma(\tau)c^*_{-\sigma}(\tau)c_{-\sigma}(\tau), \qquad (6)$$

where we used a mixed time/frequency convention for Grassmann variables c_σ, $c^\star_\sigma$. In the presence of binary alloy disorder, the single impurity problem has to be solved twice in each self-consistency loop. Averages over the randomness are obtained by [15,23,24]

$$\langle\cdots\rangle_{\rm dis} = \int d\epsilon P(\epsilon)(\cdots). \qquad (7)$$

Due to the local nature of the theory and the arithmetic averaging of the physical one-particle quantities, Anderson localization is not captured [25,26].

An asymmetric density of states is known to stabilize ferromagnetism in the one-band Hubbard model for moderate values of U [8,12,13]. Therefore, we use the density of states of the fcc-lattice in infinite dimension [27],

$$N^0(\epsilon) = \frac{\exp[-\frac{1+\sqrt{2}\epsilon}{2}]}{\sqrt{\pi(1+\sqrt{2}\epsilon)}}. \qquad (8)$$

This density of states has a square root singularity at $\epsilon = -1/\sqrt{2}$ and vanishes exponentially for $\epsilon \to \infty$. In the following, the second moment of the density of states is used as the energy scale and is normalized to unity. Since

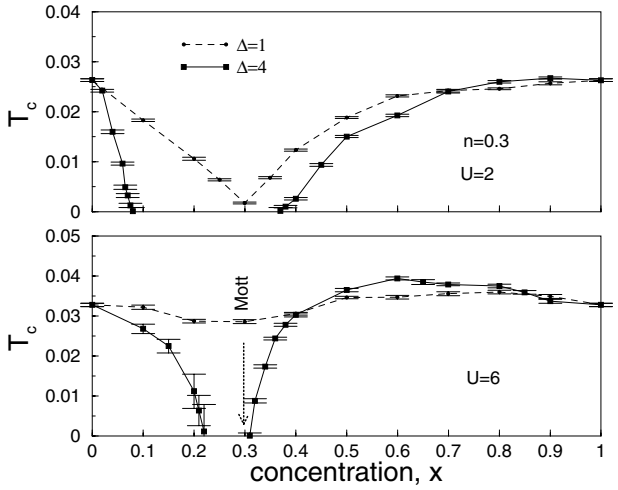

Fig. 1. Curie temperature as a function of alloy concentration x at $U = 2$ (upper panel) and 6 (lower panel) for $n = 0.3$ and disorder $\Delta = 1$ (dashed lines) and 4 (solid lines).

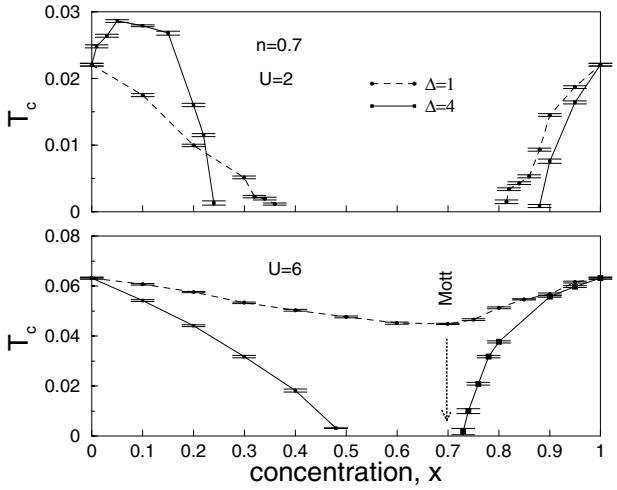

Fig. 2. Curie temperature as a function of alloy concentration x at $U = 2$ (upper panel) and 6 (lower panel) for $n = 0.7$ and disorder $\Delta = 1$ (dashed lines) and 4 (solid lines).

the same density of states has been used earlier in references [12,16] we are able to compare the specific numerical results.

The one-particle Green function in equation (4) is determined by solving the DMFT equations iteratively [12,13] using Quantum Monte-Carlo simulations with the Trotter slice $\Delta\tau = 1/4$ [28]. Since we are mostly interested in qualitative behavior of T_c vs. x at different U, n, and Δ, we do not perform the extrapolation of the results to $\Delta\tau \to 0$. Curie temperatures are obtained by the divergence of the homogeneous magnetic susceptibility explicitly implying that the ferromagnetic phase transitions are of the second order [12,29,30].

3 Results for isoelectronic alloys

3.1 Curie temperature

The Curie temperature as a function of alloy concentration exhibits very rich and interesting behavior as is documented in Figures 1 and 2. It is usually expected that $T_c(x)$ is suppressed in disordered systems. This indeed is found for most cases when x is varied between zero and one. However, at some concentrations and certain values of U, Δ and n, the Curie temperature is enhanced above the corresponding value for the $x = 0$ (1) case. This is shown in both panels of Figure 1 for $0.4 \lesssim x \lesssim 0.9$ and in the upper panel of Figure 2 for $0 \lesssim x \lesssim 0.2$. The relative increase of T_c can be as large as 25%, as is found for $x \approx 0.1$ at $n = 0.7$, $U = 2$ and $\Delta = 4$ (upper panel of Fig. 2).

This unusual enhancement of T_c is caused by three distinct features of interacting electrons in the presence of binary alloy disorder:[16]

i) The Curie temperature in the non-disordered case $T_c^{\rm p} \equiv T_c(\Delta = 0)$, depends non-monotonically on band filling n. Namely, $T_c^{\rm p}(n)$ has a maximum at some filling $n = n^*(U)$, which increases as U is increased [12]; see also our schematic plots in Figure 3.

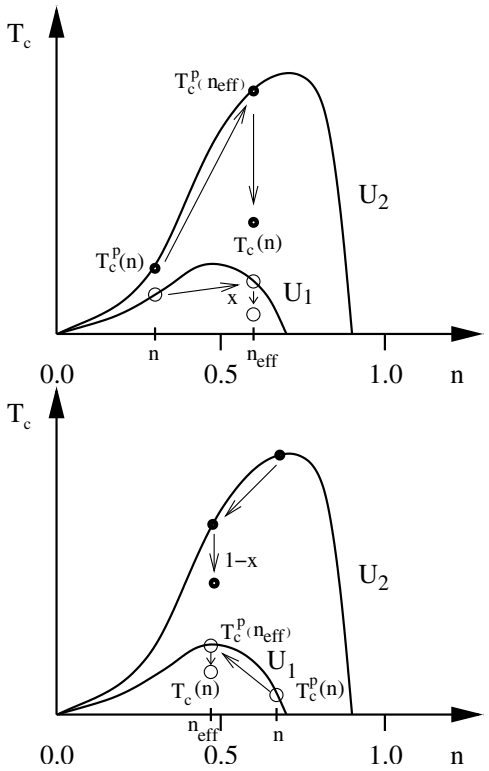

Fig. 3. Schematic plots explaining the filling dependence of T_c for interacting electrons with strong binary alloy disorder. Curves represent $T_c^{\rm p}$, the Curie temperature for the pure system, as a function of filling n at two different interactions $U_1 \ll U_2$ [12]. Upper panel: For $n \lesssim x$, T_c of the disordered system can be obtained by transforming the open (for U_1) and the filled (for U_2) point from n to $n_{\rm eff} = n/x$, and then multiplying $T_c^{\rm p}(n/x)$ by x as indicated by arrows. One finds $T_c(n) < T_c^{\rm p}(n)$ for U_1, but $T_c(n) > T_c^{\rm p}(n)$ for U_2. Lower panel: For $n \gtrsim x$, T_c of the disordered system can be obtained by transforming $T_c^p(n)$ from n to $n_{\rm eff} = (n-2x)/(1-x)$, and then multiplying $T_c^{\rm p}[(n-2x)/(1-x)x]$ by $1-x$ as indicated by arrows. One finds $T_c(n) > T_c^{\rm p}(n)$ for U_1, but $T_c(n) < T_c^{\rm p}(n)$ for U_2.

ii) As was described above, in the alloy disordered system the band is split when $\Delta \gg W$. As a consequence, for $n < 2x$ and $T \ll \Delta$ electrons occupy only the lower alloy subband and for $n > 2x$ both the lower and upper alloy subbands are filled. In the former case the upper subband is empty while in the later case the lower subband is completely full. Effectively, one can therefore describe this system by a Hubbard model mapped onto the either lower or the upper alloy subband, respectively. The second subband plays a passive role. Hence, the situation corresponds to a *single* band with the *effective* filling $n_{\rm eff} = n/x$ for $n < 2x$ and $n_{\rm eff} = (n-2x)/(1-x)$ for $n > 2x$. It is then possible to determine T_c from the phase diagram of the Hubbard model without disorder [12].

iii) The disorder leads to a reduction of $T_c^{\rm p}(n_{\rm eff})$ by a factor $\alpha = x$ if the Fermi level is in the lower alloy subband or $\alpha = 1 - x$ if it is in the upper alloy subband, i.e. we find

$$T_c(n) \approx \alpha T_c^{\rm p}(n_{\rm eff}), \tag{9}$$

when $\Delta \gg W$ (c.f. Appendix). Hence, as illustrated in Figure 3, T_c can be determined by $T_c^{\rm p}(n_{\rm eff})$. Surprisingly, then, it follows that, for suitable U and n Curie temperature of a disordered system can be higher than that of the corresponding non-disordered system [cf. Fig. 3].

The explanation of the $T_c(x)$ enhancement, given above, is supported by a detailed analysis how T_c changes when Δ increases at fixed x. The numerical results are shown in Figure 4 at $x = 0.1$ and $n = 0.7$. Examples at $x = 0.5$ already have been presented in reference [16]. For $n > 2x$ (results in Fig. 4 corresponds to this regime) the Curie temperature initially decreases upon increasing Δ from zero. However, when $\Delta \gtrsim U$ the trend is inverted and T_c increases, finally saturating. At $\Delta \sim U$ the alloy band splitting becomes effective, changing the behavior of T_c versus Δ. As shown in Figure 4, only for small U the Curie temperature is elevated above the value at $\Delta = 0$. This is strongly related to the non-monotonic dependence of $T_c^p(n)$, and in particular to the fact that its maximum changes with U. Namely, as is illustrated in the lower panel of Figure 3, only at small interactions $T_c^p(n_{\rm eff}) > T_c^p(n)$, which is a necessary condition for the enhancement of T_c by disorder. In the $n < 2x$ case, on the other hand, the necessary condition $T_c^p(n_{\rm eff}) > T_c^p(n)$ for an enhancement of T_c implies that the interaction must be strong [16].

3.2 Magnetization and Curie constant

The two different cases $n < 2x$ and $n > 2x$ (when $\Delta \gg W$) should correspond to two different behaviors of a saturated magnetization, i.e. the magnetization for $T \to 0$. Namely, in the first case only the lower alloy subband is occupied and the magnetization $M \equiv \langle \hat{n}_\uparrow \rangle - \langle \hat{n}_\downarrow \rangle = n$, where $\langle \hat{n}_{\uparrow,\downarrow} \rangle$ are the average numbers of electrons with spin up or down. However, in the second case $M = n - 2x$ since the lower alloy subband is split off and fully occupied by the electrons with two spin species, thereby being magnetically neutral.

In order to confirm this physical picture we calculate the magnetization $M(T)$ as a function of temperature.

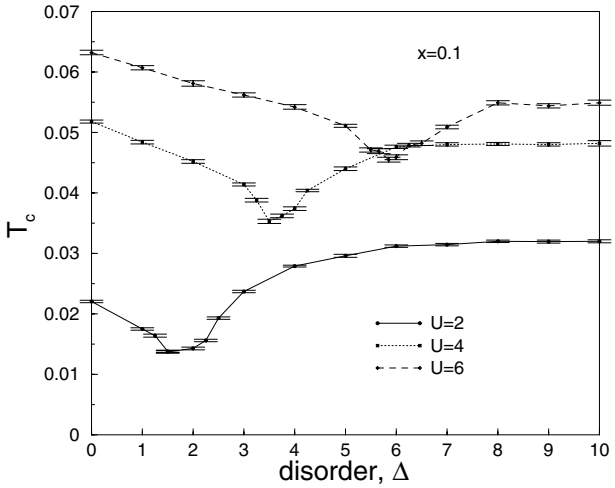

Fig. 4. Changes of the Curie temperature with disorder Δ at $x = 0.1$ and $n = 0.7$ for different interactions U.

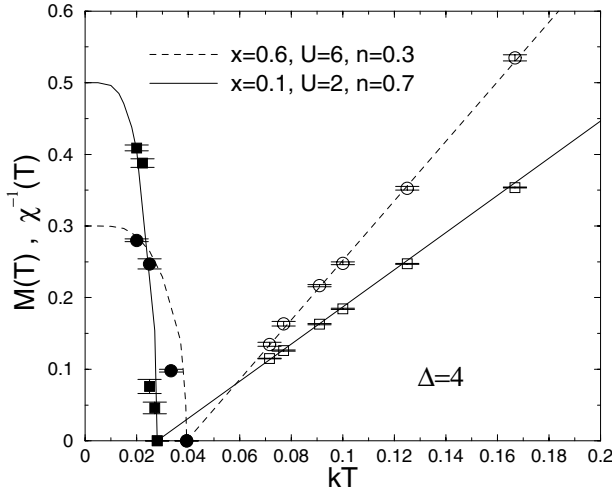

Fig. 5. Magnetization and inverse static susceptibility at: $x = 0.6$, $n = 0.3$ and $U = 6$ (circles and dashed lines), and $x = 0.1$, $n = 0.7$ and $U = 2$ (squares and solid lines). In both cases $\Delta = 4$.

The resultant magnetizations together with the inverse static susceptibilities $\chi^{-1}(T)$ are presented in Figure 5 for two cases: i) $x = 0.6$, $n = 0.3$, and $U = 6$ (filled and open circles), corresponding to $n < 2x$ case, and ii) $x = 0.1$, $n = 0.7$, and $U = 2$ (filled and open squares) corresponding to $n > 2x$ instance. At both parameter sets T_c is enhanced by the alloy band splitting ($\Delta = 4$). The numerically calculated magnetization (filled circles and squares) follow very closely the theoretical Brillouin curves (dashed and solid lines) [31,32]. The magnetization data, shown in Figure 5, are consistent with our conjecture that the saturated magnetization should be: $M = n = 0.3$ in case (i), whereas $M = n - 2x = 0.5$ in case (ii).

Two interesting observations are made: Firstly, in the case (ii) (with $n > 2x$), the presence of disorder increases T_c while the saturated magnetization is suppressed below its value at $x = 0$. In other words, the disordered system becomes a weaker ferromagnet but with higher T_c. Secondly, although the correlated electrons in the disordered

system are itinerant, the magnetization $M(T)$ is well reproduced by the Brillouin curve, albeit formally this curve is derived for localized moments [12]. The last observation calls for an analytical proof within DMFT analogous to that already given for the linear behavior of the inverse susceptibility [29].

Within DMFT the uniform spin susceptibility for a systems with paramagnet-ferromagnet phase transition obeys the Curie-Weiss law $\chi(T) = C/(T - T_c)$ [29], where C is a Curie constant. The same Curie-Weiss law is also derived with a mean-field theory for localized magnetic moments and in this case the Curie constant is directly proportional to the saturated magnetization. To check if similar relation holds for itinerant electron system within DMFT we compute the Curie constants obtaining: $C_1 = 0.240 \pm 0.002$ in the case (i), and $C_2 = 0.385 \pm 0.001$ in the case (ii). It turns out that the ratio $C_1/C_2 = 0.623 \pm 0.005$ is very close to the ratio of saturated magnetizations $0.3/0.5 = 0.6$. This result provides a new interpretation of the Curie constant within DMFT, i.e. C is proportional to the saturated magnetization, similarly as in localized magnetic moment theory. In addition this finding corroborates our initial conjecture regarding saturated magnetization in two physically different cases $n < 2x$ and $n > 2x$ at large Δ.

3.3 Metal-insulator transition

Upon increasing U and Δ, the Mott-Hubbard MIT occurs at the electronic filling $n = x$ [16,17]. Such MIT can also be encountered by varying x. This MIT will be called an *alloy concentration controlled Mott transition*. Approaching a correlated insulator the itinerant ferromagnetism is also suppressed due to localization of the electrons. Using linearized DMFT [33] it was estimated [17] that when $\Delta \to \infty$ the critical interaction $U_c \approx 6\sqrt{x}$. Such estimation leads to $U_c \approx 3.3$ for $n = 0.3$ (Fig. 1), and to $U_c \approx 5$ for $n = 0.7$ (Fig. 2). This means that at $\Delta = 4$ and $U = 6$ (lower panels in Figs. 1 and 2) the Mott-Hubbard MIT is possible at $x = n$.

4 Non-isoelectronic alloy

In many alloys the change in the concentration x alters the electron density n. In this section we investigate $T_c(x)$ when x and n are varied simultaneously. The results presented in Figure 6 are obtained under the assumption that $x = 2n$. When $x = 0$ the band is empty (the system is a band insulator). Upon increasing x from zero to one, the band filling increases from zero to one-half (quarter filled band). This model realization would correspond to the physical situation in $Fe_{1-x}Co_xS_2$ alloy if the number of states in e_g band is normalized to one. Of course, this analogy should not be stressed too far since in our model an important exchange interaction (Hund's coupling) is absent.

As shown in Figure 6 the presence of disorder at weak interaction always suppresses the Curie temperature with respect to the non-disorder case. However, at large U and

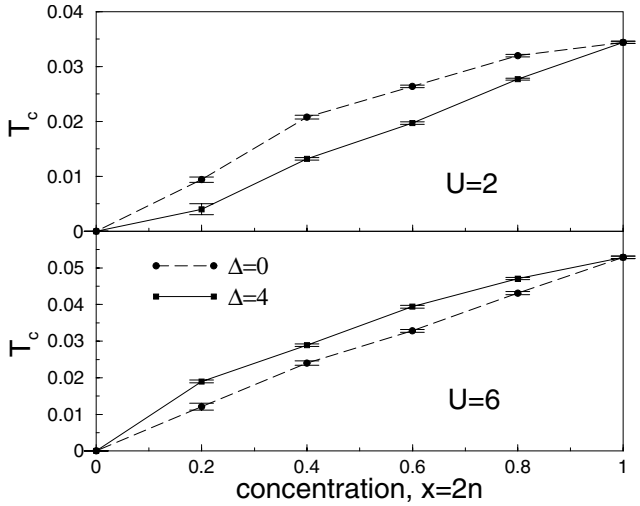

Fig. 6. Behavior of the Curie temperature for $U = 2$ (upper panel) and 6 (lower panel) when the change of electron filling n is associated with the change in the alloy concentration x. At large U the Curie temperature is enhanced in the disorder system.

$\Delta \gtrsim 1$ the Curie temperature is larger than that in the pure case at the same filling.

This difference again can be understood on the basis provided by the scheme depicted in Figure 3. In the present case $n < 2x$ for all x, and only the lower alloy subband plays a role in the effective description at large Δ. In this limit this subband is effectively filled with $n_{\text{eff}} = n/x = 1/2$ electrons. Using the same arguments as in the upper panel in Figure 3 we see that $T_c(x)$ is enhanced only for large U.

5 Conclusions

In the present paper we studied the one-band Anderson-Hubbard model with binary alloy disorder showing that the Curie temperature in such alloyed correlated electron system can reach higher values than those in the non-disorder system. We also identified and discussed the metal-insulator transition at non-integer fillings.

Regarding the physical systems, it is now of great importance to extend the one-band Hubbard model with alloy disorder to a multi-band case and formulate the adequate version of DMFT for solving this problem. It is very interesting which aspect of the ferromagnetism in one-band alloy are generic and will be present in multi-band case.

We thank R. Bulla and D. Vollhardt for useful discussions and Ch. Leighton for communication on $Fe_{1-x}Co_xS_2$ pyrite. This work was supported in part by the Sonderforschungsbereich 484 of the Deutsche Forschungsgemeinschaft. We thank the Institute of Physics of the University of Augsburg for hospitality and for being able to make use of their computer resources. Financial support of KB through KBN-2 P03B 08 224 is also acknowledged.

Appendix A: Hartree-Fock theory

Within the Hartree-Fock approximation one can find analytically that in the strong disordered limit $\Delta \gg W$ the self-energy has the form

$$\Sigma_{n\sigma} = \sigma\frac{UM}{4} + (1-2x)\frac{\Delta}{2} + \frac{x(1-x)\Delta^2}{z - \frac{\sigma UM}{4} - \frac{2-x}{2}\Delta}, \quad (10)$$

where M is the magnetization density. This self-energy leads to the splitting of the density of states with x and $1-x$ of the initial states in each alloy subband. Since the integrated function in the equation for $T_c^{\rm HF}$ is peaked at $\omega = \mu$, only one of the subband gives contribution to evaluate $T_c^{\rm HF}$. As a result, $T_c^{\rm HF} \approx \alpha T_c^{{\rm HF}\,p}$, where $\alpha = x$ or $1-x$, as introduced in Section 2. Although in DMFT one cannot find analytically the corresponding self-energy, the splitting of the density of states also appears and only one of the subbands contributes in the equation for T_c. In analogy to the Hartree-Fock approximation, we assume that T_c is reduced by α with respect to T_c^p, which we find to be valid even at strong interaction.

References

1. M. Imada, A. Fujimori, Y. Tokura, Rev. Mod. Phys. **70**, 1039 (1998)
2. E. Dagotto, T. Hotta, A. Moreo, Phys. Rep. **344**, 1 (2001)
3. G. Cao et al., `cond-mat/0409157`
4. S. Yeo et al., Phys. Rev. Lett. **91**, 046401 (2003)
5. V.I. Anisimov et al., Phys. Rev. Lett. **89**, 257203 (2002)
6. I. Zutic, J. Fabian, S. Das Sarma, Rev. Mod. Phys. **76**, 323 (2004)
7. T. Dietl, Semicond. Sci. Technol. **17**, 377 (2002)
8. D. Vollhardt, N. Blümer, K. Held, M. Kollar, in *Band-Ferromagnetism*, edited by K. Baberschke, M. Donath, W. Nolting, Lecture Notes in Physics, Vol. 580 (Springer, Berlin, 2001), p. 191
9. A. Georges, G. Kotliar, W. Krauth, M.J. Rozenberg, Rev. Mod. Phys. **68**, 13 (1996)
10. Th. Pruschke, M. Jarrell, J.K. Freericks, Adv. Phys. **44**, 187 (1995)
11. D. Vollhardt, *Correlated Electron Systems*, Vol. 9, edited by V.J. Emery (World-Scientific, Singapore, 1993), p. 57
12. M. Ulmke, Eur. Phys. J. B **1**, 301 (1998)
13. J. Wahle, N. Blumer, J. Schlipf, K. Held, D. Vollhardt, Phys. Rev. B **58**, 12749 (1998)
14. A.I. Lichtenstein, M.I. Katsnelson, G. Kotliar, Phys. Rev. Lett. **87**, 067205 (2001)
15. B. Velicky, S. Kirkpatrick, H. Ehrenreich, Phys. Rev. **175**, 747 (1968)
16. K. Byczuk, M. Ulmke, D. Vollhardt, Phys. Rev. Lett. **90**, 196403 (2003)
17. K. Byczuk, W. Hofstetter, D. Vollhardt, Phys. Rev. B **69**, 045112 (2004)
18. D.I. Bardos, J. App. Phys. **40**, 1371 (1969); M. Pratzer, H.J. Elmers, Phys. Rev. Lett. **90**, 077201 (2003)
19. I. Turek, J. Kudrnovsky, V. Drchal, P. Weinberger, Phys. Rev. B **49**, 3352 (1994)
20. H.S. Jarrett et al., Phys. Rev. Lett. **21**, 617 (1968); G.L. Zhao, J. Callaway, M. Hayashibara, Phys. Rev. B **48**, 15781 (1993); S.K. Kwon, S.J. Youn, B.I. Min, Phys. Rev. B **62**, 357 (2000); T. Shishidou, A.J. Freeman, R. Asahi, Phys. Rev. B **64**, 180401(R) (2001); J.F. DiTsua et al., `cond-mat/0306541`
21. M.B. SilvaNeto, A.H. CastroNeto, D.J. Mixson, J.S. Kim, G.R. Stewart, Phys. Rev. Lett. **91**, 257206 (2003)
22. W. Metzner, D. Vollhardt, Phys. Rev. Lett. **62**, 324 (1989)
23. R. Vlaming, D. Vollhardt, Phys. Rev. B **45**, 4637 (1992); V. Janiš, D. Vollhardt, Phys. Rev. B **46**, 15712 (1992)
24. M. Ulmke, V. Janiš, D. Vollhardt, Phys. Rev. B **51**, 10411 (1995)
25. P.W. Anderson, Phys. Rev. **109**, 1492 (1958)
26. For a variant of DMFT where the Anderson localization is included by using geometric averages see: V. Dobrosavljevic et al., Eur. Phys. Lett. **62**, 76 (2003); K. Byczuk, W. Hofstetter, D. Vollhardt, Phys. Rev. Lett. **94**, 056404 (2005)
27. E. Müller-Hartmann, in *V Symposium "Physcs of Metals"*, edited by E. Talik, J. Szade (Silesian University-Poland, 1991), p. 22
28. J.E. Hirsch, R.M. Fye, Phys. Rev. Lett. **56**, 2521 (1986)
29. K. Byczuk, D. Vollhardt, Phys. Rev. B **65**, 134433 (2002)
30. The high and moderate temperature data for the inverse susceptibility, obtained from the Quantum Monte-Carlo simulations, are extrapolated by the linear function to lower temperatures according to the Curie-Weiss law [29]. This allows us to determine even very low T_c values
31. The Brillouin curves follow from solutions of the self-consistent equation $M(T)/M_s = \tanh[T_c M(T)/(TM_s)]$, where M_s are assumed to be saturated magnetizations and T_c are earlier computed Curie temperatures
32. Due to the Monte-Carlo method it is extremely difficult to perform calculations at lower temperatures then those presented in Figure 5
33. R. Bulla, M. Potthoff, Eur. Phys. J. B **13**, 257 (2000)